



HAL
open science

Response of an ocean-atmosphere climate model to Milankovic forcing

E. S. Posmentier

► **To cite this version:**

E. S. Posmentier. Response of an ocean-atmosphere climate model to Milankovic forcing. *Nonlinear Processes in Geophysics*, 1994, 1 (1), pp.26-30. hal-00301714

HAL Id: hal-00301714

<https://hal.science/hal-00301714>

Submitted on 18 Jun 2008

HAL is a multi-disciplinary open access archive for the deposit and dissemination of scientific research documents, whether they are published or not. The documents may come from teaching and research institutions in France or abroad, or from public or private research centers.

L'archive ouverte pluridisciplinaire **HAL**, est destinée au dépôt et à la diffusion de documents scientifiques de niveau recherche, publiés ou non, émanant des établissements d'enseignement et de recherche français ou étrangers, des laboratoires publics ou privés.

Response of an ocean-atmosphere climate model to Milankovic forcing

E.S. Posmentier

Southampton College of Long Island University, Southampton, NY 11968, USA

Received 11 February 1994 - Accepted 2 March 1994 - Communicated by A.D. Kirwan

Abstract. There is considerable evidence in support of Milankovic's theory that variations in high-latitude summer insolation caused by Earth orbital variations are the cause of the Pleistocene ice cycles. The enigmatic discrepancy between the spectra of Milankovic forcing and of Pleistocene climate variations is believed to be resolved by the slow, nonlinear response of ice sheets to changes in solar seasonality. An experiment with a preliminary version of a 14-region atmosphere/snow/upper ocean climate model demonstrates that the response of the ocean-atmosphere system alone to Milankovic forcing is capable of driving ice cycles with the observed spectrum. This occurs because of the highly nonlinear response of both the thermal seasons and the annual mean temperature to solar seasons, which is caused in turn by the highly nonlinear feedback between temperature and snow and sea ice.

strongest period of climate variations during the last million years is 100 kyr, with much weaker variations around 21 kyr (Imbrie, 1985) -- precisely the opposite of the orbital effect on solar seasonality!

Several different mechanisms have been suggested as possible resolutions of the discrepancy between the spectra of the "Milankovic forcing" and of observed climate variations. One widely accepted suggestion is that nonlinear climate interactions might resolve this discrepancy (Hays *et al.*, 1976), and that this nonlinear interaction might be the slow, nonlinear response of continental ice sheets to variations of the solar seasons. This suggestion was further developed by Imbrie and Imbrie (1980). It has been extended by use of a cryodynamic model (Polard, 1982), a nonlinear two-component model (Posmentier, 1990) and a nonlinear three-component model (Saltzman *et al.*, 1984).

In the process of testing and verifying a preliminary version of a medium-dimensional atmosphere/snow/upper ocean climate model, it was found that very small adjustments to the earth's orbital parameters, which appear in the algorithm for time- and latitude-dependent insolation, can result in significant changes in climate, and that their effects on climate are strongly nonlinear. These observations suggested a question: can this preliminary climate model, which includes feedbacks among atmospheric temperatures and humidities, clouds, land and sea surface temperatures, snow, and sea ice, but not the cryosphere, biosphere, or CO₂, respond to Milankovic forcing in the same manner as observed climate variations? A model experiment to study this question is reported on here. Of course, even if dynamics of the cryosphere, the biosphere, and CO₂ are not necessary to explain the existence of glacial cycles, as indicated by the experiment, they are still primary factors in determining characteristics of the cycles.

1. Introduction

It has long been thought by many climatologists that the Pleistocene glacial cycles may have been caused by variations in the earth's orbital parameters (Milankovic, 1941). Although these orbital parameters have little effect on the solar constant, they do influence the seasonality of insolation at high latitudes, which may in turn cause climate shifts. Hays *et al.* (1976), while supportive of this hypothesis, recognized a significant discrepancy between the solar forcing spectrum and the observed climate spectrum. The three dominant variations of the earth's orbit are in the phase of the equinox relative to aphelion (precession, with a cycle about 21 kyr in period), in the tilt (nutations, with a period of approximately 40 kyr), and in the eccentricity (with a period close to 100 kyr). Of these, the precession has the largest effect on the seasonality of high latitude insolation. The variations of eccentricity have a 100 kyr modulating effect on the 21 kyr variations caused by the precession. This causes a splitting of the 21 kyr peak in the spectrum of solar seasonality, but contributes very little energy to the spectrum at 100 kyr. In contrast, it is indicated by geological evidence that the

2. The Model

The preliminary model (Fig. 1) divides the Earth into seven zones -- a dry subtropical zone, a wet temperate

zone, a polar zone in each hemisphere, and an intertropical convergence zone. Each zone is divided between land and ocean regions, resulting in a total of 14 regions. Within each region, there is a surface layer (solid land or ocean mixed layer), and two atmospheric layers (1000-500mb and above 500mb). The only surface variable is temperature, but snow (on land) and ice (on the ocean) areas are implicit variables in temperature-dependent albedos. Temperature, specific humidity, and cloud area are variables in each atmospheric layer.

REGIONS AND LAYERS OF CLIMATE MODEL

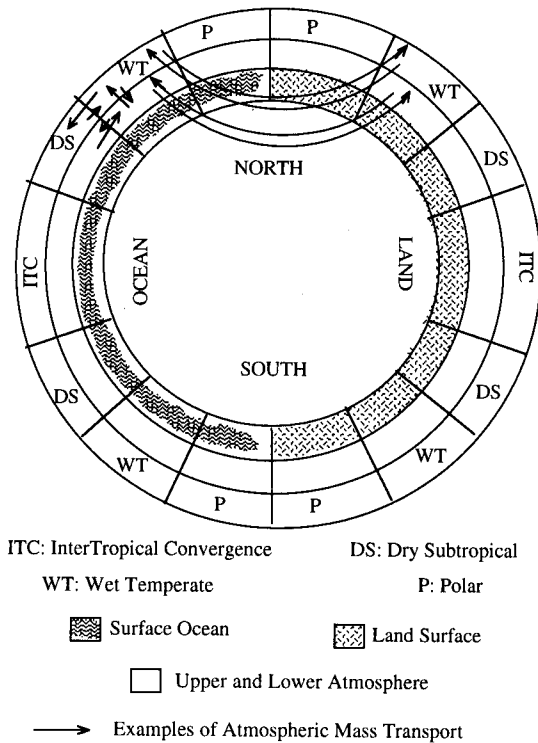


Fig 1. The model's seven zones with one land and one ocean region in each, and with a surface layer -- either solid land or ocean mixed layer -- and two atmospheric layers in each region. Arrows represent examples of mass transports of air, which effect heat and water vapor transports in both directions across interfaces between adjacent atmospheric elements.

Temperatures are governed by finite element heat balance equations. These include radiative, advective, latent, and sensible fluxes. The radiative fluxes include solar absorption, scattering or reflection, and transmission, based on independently-specified coefficients for the surface, and for clear and cloudy lower and upper layers (see Table I.) They also include emission and absorption for the "black" part of the terrestrial infrared, which is 91% of the total infrared. The remaining 9% of the infrared is "gray", with partial transmission through the atmosphere (see Table I.) Advective transport in both directions across each interface between adjacent atmospheric elements is computed based on meridional, zonal, and vertical bi-directional winds. The winds are specified consistently

with the general circulation, conservation of mass, and Reynold's transports. Latent fluxes are determined by the evaporation and precipitation rates, discussed below, and the surface sensible heat flux is computed using a Bowen's ratio of 1.0 on land and 0.5 on the ocean..

Table 1. Radiation Parameters

P (mb)	Clear Air		Cloudy Air	
	1000-500	<500	1000-500	<500
Solar absorption	0.09	0.09	0.10	0.08
Solar scattering	0.02	0.05	0.85	0.75
Gray IR absorption	0.14	0.07	0.90	0.90
Black IR absorption	1.00	1.00	1.00	1.00

Specific humidities are governed by finite element water balance equations. These include evaporation into lower layer elements, advective transport in both directions across each interface between adjacent atmospheric elements, and precipitation (discussed below). Evaporation is assumed to be proportional to the difference between the saturation specific humidity at the surface temperature and the specific humidity in the lower layer of the atmosphere in the same region. The constants of proportionality land and ocean are $2.5 \cdot 10^{-3}$ and $5.0 \cdot 10^{-3}$ $\text{kg/m}^2/\text{s}$, respectively.

For each atmospheric element, the saturation specific humidity q_s is calculated for air originating at the element's average pressure, temperature, and specific humidity, after ascending at a velocity equal to the greater of the pair bi-directional vertical velocities, for a period equal to the residence time in the element. The potential precipitation per unit mass of air is $(q - q_s) \cdot H(q - q_s)$, where H is the Heaviside function. The precipitation r used in the conventional "all-or-none" approach is this potential precipitation. In this model, r is an arbitrarily smoothed version of this potential precipitation, given by

$$r = (1/s) \ln[\exp(s \cdot (q/q_s - a)) - \exp(-sa) + 1] \quad (1)$$

where s is a smoothing parameter and a is the critical value of q/q_s . As $s \rightarrow \infty$, r approaches the unsmoothed potential precipitation. The constant a is close to unity, and represents the value of q/q_s at which precipitation begins to grow significantly. In the experiment reported here, $s=4.0$ and $a=1.0$.

The fractional area of cloudiness c in an atmospheric element would be $H(q - q_s)$ in the "all-or-none" approach, but this model uses a smoothed version

$$c = 0.5x \cdot \exp(tx) / [x \cdot \exp(tx) + b \cdot \exp(t)] \quad (2)$$

where x is the ratio $r(q)/r(aq_s)$, t is an arbitrary smoothing parameter, and b is a critical value of x . As $t \rightarrow \infty$, c approaches $H(q - q_s)$. The constant b is close to unity, and

represents the value of x at which the cloud area begins to grow significantly. In the experiment reported here, $t=4.0$ and $b=1.0$.

In summary, the model is comprised of 14 regions (land and ocean in each of 7 zones), with 5 governing equations for each (conservation of heat for the surface and both layers of the atmosphere, and of water water for both layers of the atmosphere). The time derivatives of temperature and specific humidity in the 56 atmospheric equations are set to zero. These equations are then solved by iteration for the variables describing an atmosphere in equilibrium with the surface.

The 14 surface heat conservation equations are used to evaluate the time derivatives of the surface temperatures, assuming surface heat capacities corresponding to 2m of water for land, and to latitude-dependent mixed layer depths between 20-40m for the ocean. These 14 warming rates depend on the radiative fluxes and latent and sensible heat fluxes, which depend in turn on the atmospheric variables governed by the 56 atmospheric balance equations. The 14 warming rates are integrated using 128 time steps per year. The fourth-order Runge-Kutta method is used for the first four steps, after which the fourth-order Adams-Bashforth/Adams-Moulton predictor-corrector method is used.

A preliminary "tuning" of the model was done before the experiment reported here. All radiation coefficients (Table I) were adjusted to agree with published radiation budgets, and other parameters were adjusted by comparison of results with observations of seasonal and meridional surface temperatures, and meridional variations of cloudiness and precipitation. There are more independent comparisons to be made than there are model parameters to which the results are sensitive, so the goodness of comparison confirms the completeness of the physical processes included in the model. Support for this assertion by a systematic comparison between observations and model results, however, is reserved for another paper.

3. Results of Model Experiment

A numerical experiment was performed to test of the hypothesis that Milankovic forcing of the climate system can produce the observed climate response without interactions with the cryosphere or the biosphere. For purposes of this experiment, the three slowly varying earth orbital parameters were assumed to follow

$$\text{tilt}=23.0+1.5*\sin(2*\pi*t/16.5)/40 \quad (3)$$

$$\text{eccentricity}=.05+.05*\sin(2*\pi*t/100) \quad (4)$$

$$\text{perihelion}=365*t/21+171.25 \quad (5)$$

where "tilt" is the tilt of the earth's axis of rotation in degrees, "eccentricity" is the eccentricity of the earth's orbit, "perihelion" is the time lag in days from aphelion until summer solstice, and t is time in kyr. The periods and amplitudes of these functions match the actual orbit of the earth, but the origin of time is arbitrary.

Using the orbital parameters from Equations (3)-(5) for $t=0$, the model was run until an annual limit cycle was reached. This required 16 years. Then, t was advanced to 1.5 kyr, the orbital parameters were re-evaluated, and the model was run until a new annual limit cycle was reached. This was iterated until t reached 200 kyr. The property of insolation believed by Milankovic to be crucial to the growth and decay of continental glaciation is the "summer" insolation for the 6-month period from vernal to autumnal equinox reaching the top of the atmosphere at 65°N . The variation of summer insolation at 65°N during this numerical experiment is shown in the upper curve of Fig. 2. It is dominated by a 21 kyr oscillation caused by precession, with a 100 kyr modulation caused by variations of eccentricity, and is essentially identical to similar reconstructions based on precise earth orbits (for example, Vernekar, 1971).

The maximum surface temperature during the annual cycle, in the Northern Hemisphere wet temperate ocean region, referred to below as "T", is shown in the center curve in Fig. 2. T is virtually in phase with summer insolation. But compared to the insolation, its distribution about its mean is strikingly asymmetric -- *i.e.*, the maxima of T exceed its mean by far more than the minima fall below the mean.

CLIMATE RESPONSE TO ORBITAL VARIATIONS

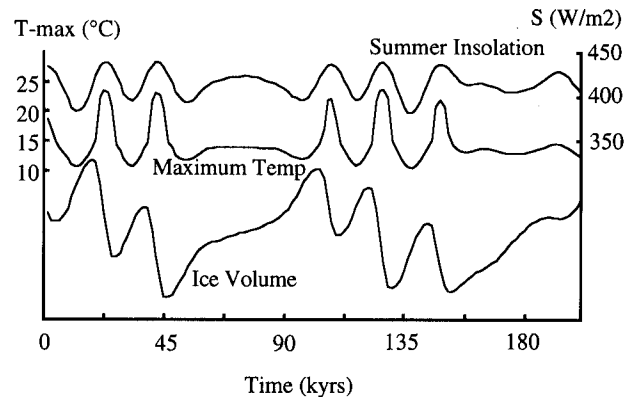


Fig. 2. The average insolation at 65°N during the six summer months -- *i.e.*, the Milankovic forcing -- for the 200 kyr numerical experiment (upper curve); the annual maximum surface temperature in the northern wet temperate ocean region (middle curve); and ice volume, in arbitrary units (lower curve).

Some insight into the cause of the asymmetric distribution of T can be gained from a direct comparison of T with insolation (Fig. 3), which shows an extremely sharp increase in slope near an insolation of 430 W/m^2 . This suggests that there may be a positive feedback between solar seasons and thermal seasons which is operative only if summer insolation at 65°N exceeds 430 W/m^2 . In fact, the feedback between temperature and snow and sea ice, caused by albedo variations, have precisely this effect. As summer insolation increases compared to an initially small value, during millennia of increasing but weak solar seasonality in the Northern Hemisphere, a small increase in summer temperature results, but the length of the snow and

sea ice season is not significantly affected. As summer insolation increases further, beyond 430 W/m^2 , the further increase in summer temperature begins to cause a decrease in the length of the snow and ice season, decreasing the albedo, and reinforcing the temperature increase.

The annual mean temperature of the wet temperate ocean region (not shown) follows the same pattern as T , within a range of about 6°C , in agreement with observations (Ruddiman and McIntyre, 1984, and Rind and Peteet, 1985). It is remarkable that variations only in solar seasonality, but not in the solar constant, can cause the annual mean temperature to vary this much. This is caused by the albedo feedback, and the related strong nonlinearity in the effect of solar seasonality on T . The dependence of annual average temperature on seasonality is often overlooked by models of long-term climate change. However, its importance has been recognized by Crowley *et al.* (1986) and by Kagan *et al.* (1988). The critical role of snow in similar inter-annual climate variations has been studied by Adem (1981).

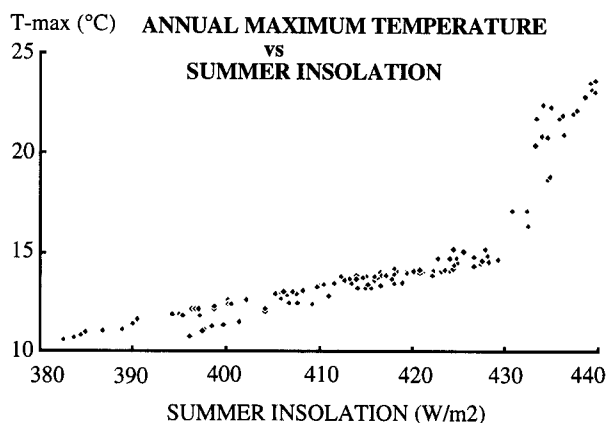


Fig. 3. The annual maximum surface temperature in the northern wet temperate ocean region, from Fig. 2, as a function of the Milankovic forcing.

The simplest possible model for ice volume would be a growth rate directly proportional to $T - T^a$, where T^a is the long-term average T . Ice volume variation based on this minimal ice model is shown in the lowest curve in Fig. 2. Ice volume variation includes a 21 kyr component, also present in both summer insolation and T , but in addition, it has the essential, enigmatic feature of observations -- it is dominated by a 100 kyr component, which is not present in the Milankovic forcing (upper curve) except as a modulation. In addition, it replicates the observed features of rapid, episodic retreats separated by slower, steadier advances.

Another aspect of the model's response to Milankovic forcing may be relevant to observed behaviour of the climate. Other model experiments show that the 100 kyr periodicity in ice volume, and the nonlinearities which cause it, are very sensitive to some model parameters and to the solar constant. For slightly different scenarios, the discontinuity in slope at 430 W/m^2 in Fig. 3 is shifted to much larger (or smaller) values of summer insolation, out

of the range of variability of solar seasonality. Under such conditions, the climate will be always weakly sensitive (or always strongly sensitive) to solar variations, but linearly sensitive in either case. These results correspond to ice cycles which are weak (or strong) but with 20 kyr periodicities in either case. In fact, precisely such weak 20 kyr variations of climate characterize the first half of the Pleistocene, and stronger 100 kyr cycles resembling the model results in Fig. 2 occurred only in the second half (Raymo *et al.*, 1989).

This model's realistic response to Milankovic forcing is entirely the result of the interactions within the atmosphere/snow/upper ocean system, excluding the dynamics of the cryosphere, the biosphere, or CO_2 . This does not imply, however, that the latter dynamics do not significantly affect global climate cycles, or that they are not independently able to respond realistically to Milankovic forcing. What the model experiment does imply is that interactions within the atmosphere/snow/upper ocean part of the global climate system are an important factor in the global climate response to Milankovic forcing. Interactions within this part of the system should be considered as a possible triggering effect or amplifying effect for cycles already known to arise from the response of the cryosphere, biosphere, and CO_2 to Milankovic forcing.

4. Conclusions

The response of the earth's climate system to long-term variations in external factors such as seasonality of high-latitude insolation is the combined effect of the atmosphere, snow, oceans, cryosphere, CO_2 , and biosphere, and their interactions. However, the model experiment described here suggests that atmosphere/snow/upper ocean dynamics alone is sufficient to account for the enigmatic, distinct difference between the spectra of Milankovic forcing and climate variations. The model climate also responds with relatively fast glacial retreats and slow advances, as observed. Furthermore, the sensitivity of these responses to model parameters suggests that strong 100 kyr ice cycles might appear and disappear on an even longer time scale, as has also been observed. It is confirmed that solar seasonality can have a strong nonlinear influence on annual-average climate. The feedback between surface temperature and snow and sea ice is critical to these results.

Acknowledgments. This research was supported by the Electric Power Research Foundation. The author is grateful for the suggestions and encouragement of N.K. Balachandran, D. Rind, B. Brody, and A. Feiner.

References

- Adem, J., Numerical simulation of the annual cycle of climate during the ice ages, *J. Geophys. Res.*, 86, 12015-1234, 1981.
- Crowley, T.J., D.A. Short, J.G. Mengel, and G.R. North, Role of seasonality in the evolution of climate during the last 100 million years, *Science*, 231, 579-584, 1986.

- Hays, J.D., J. Imbrie, and N.J. Shackleton, Variations in the Earth's orbit: pacemaker of the ice ages, *Science*, *174*, 4270, 1121-1132, 1976.
- Imbrie, J., A theoretical framework for the Pleistocene ice ages, *J. Geol. Soc. (London)*, *142*, 417-432, 1985.
- Imbrie, J., and J.Z. Imbrie, Modeling the climatic response to orbital variations, *Science*, *207*, 943-953, 1980.
- Kagan, B.A., B.A. Ryabchenko, and A.S. Safray, Seasonal variability of the ocean-atmosphere system at the maximum of the last glaciation: numerical experiments, *Izvestia, Atmos. Oc. Phys.*, *24*, 4, 251-259, 1988.
- Milankovic, M.M., *Canon of insolation and the ice age problem*, Königlich Serbische Akademie, Beograd. (English translation by the Israel Program for Scientific Translation, U.S. Dept. of Commerce and Nat. Sci. Fdn., Washington, D.C.), 1941.
- Polard, D., 1982. A simple ice sheet model yields realistic 100 kyr glacial cycles, *Nature*, *296*, 334-338.
- Posmentier, E.S., Periodic, quasiperiodic, and chaotic behaviour in a nonlinear toy climate model, *Annales Geophysicae*, *8*, 11, 781-790, 1990.
- Raymo, M.E., W.F. Ruddiman, J. Backman, B.M. Clement, and D.G. Martinson, Late Pliocene variation in northern hemisphere ice sheets and North Atlantic deep water circulation, *Paleoceanography*, *4*, 413-446, 1989.
- Rind, D., and D. Peteet, Terrestrial conditions at the last glacial maximum and CLIMAP sea-surface temperature estimates: Are they consistent?, *Quaternary Res.*, *24*, 1-24, 1985.
- Ruddiman, W.F., and A. McIntyre, Ice-age thermal response and climatic role of the surface Atlantic Ocean, 40°N to 63°N, *Geol. Soc. Amer. Bull.*, *95*, 381-396, 1984.
- Saltzman, B., A.R. Hansen, and K.A. Maasch, The late Quaternary glaciations as the response of a three-component feedback system to Earth-orbital forcing, *J. Atmos. Sci.*, *41*, 3380-3389, 1984.
- Vernekar, A.D., Long-period global variations of incoming solar radiation, *Met. Monogr.*, *12*, 34, 1-10, 1971